Conf-8208100--1

BNL--32096

BNL 32096

DE83 003723

EVIDENCE FOR EXPLICIT GLUEBALLS FROM THE REACTION $\pi^- p \to \phi\phi n$ †

S.J. Lindenbaum

Brookhaven National Laboratory, Upton, New York 11973

and

City College of New York, New York, New York 10031

NOTICE

PORTIONS OF THIS REPORT ARE ILLEGIBLE. It has been reproduced from the best available copy to permit the broadest possible availability.

Lecture presented at the 20th Course:

Gauge Interactions: Theory and Experiment

International School of Subnuclear Physics

Erice, Trapani, Italy

August 3-14, 1982

DISCLAIMER

This report was prepared as an account of work sponsored by an agency of the United States Government. Neither the United States Government nor any agency thereof, nor any of their employees, makes any warranty, express or implied, or assumes any legal liability or responsibility for the accuracy, completeness, or usefulness of any information, apparatus, product, or process disclosed, or represents that its use would not infringe privately owned rights. Reference herein to any specific commercial product, process, or service by trade name, trademark, manufacturer, or otherwise does not necessarily constitute or imply its endorsement, recommendation, or favoring by the United States Government or any agency thereof. The views and opinions of authors expressed herein do not necessarily state or reflect those of the United States Government or any agency thereof.

† This research was supported by the U.S. Department of Energy under Contract Nos. DE-AC02-76CH00016 (BNL) and DE-AC02-79ER10550A (CCNY) and the National Science Foundation under Contract No. PHY8C-09788.

MASTER

DISTRIBUTION OF THIS DOCUMENT IS UNLIMITED

EVIDENCE FOR EXPLICIT GLUEBALLS FROM THE REACTION $\pi^- p \to \phi\phi n$

S.J. Lindenbaum

Brookhaven National Laboratory, Upton, New York 11973

and City College of New York, New York, New York 10031

INTRODUCTION

In a pure Yang-Mills theory[1] where $SU(3)_c$ has local gauge symmetry, all hadrons would be glueballs[2] (i.e., multi-gluon resonances). This is due to the self-coupling of the gluons which becomes stronger with decreasing energy and color confinement.

But what do we find experimentally? The hadronic sector is dominated by $q\bar{q}$ and qqq and there is yet no prior "experimental" demonstration of the explicit existence of glueballs, although there were a number of glueball candidates and extensive discussion of them.[3-17] Thus the quarks which are a source* of particles for gluons in QCD appear to have completely taken over the hadronic sector.

Therefore finding glueballs is crucial to QCD, Grand Unification Schemes and Partial Unification Schemes which utilize $SU(3)_c$. In fact it has been the author's opinion for some time[5,6] that if we don't establish glueballs, QCD is in serious trouble. On the other hand, the explicit establishment of glueball's would indeed be a great triumph for QCD.

* Gluons are also a source of gluons due to the self-couplings in a non-Abelian Gauge Theory.

HOW DO YOU FIND GLUEBALLS?

It is obvious from prior experimental observation that if glueballs exist they are essentially masked in the vast collection of meson nonets, existing in the mass range where one would expect to find them ($\sim$ 1-3 GeV).

Pattern Recognition of a Decuplet

The direct approach is a complicated pattern recognition problem. *One must find a nonet with a glueball with the same quantum numbers near enough to the singlets in the nonet to mix with them.* Thus one would have

nonet + glueball → decuplet

with characteristic mixing and splitting (and other special characteristics of glueballs). Calculations have shown that the ideal mixing observed in a great deal of nonets would be affected in these decuplets, and pattern recognition would have to be used.[16,17] A glueball candidate of this type is the SLAC $J^{PC} = 0^{-+}$ $\iota(1440)$,[8-10,16] which could be the tenth member of a ground state 0^{-+} decuplet.* Another glueball candidate of this type is the BNL/CCNY $J^{PC} = 0^{++}$ $g_s(1240)$.[15] This would make a new 0^{++} multiplet with apparently the right characteristics: Of course one must realize that there are many other possible explanations for these states.**

Look in an OZI Suppressed Channel with a Variable Mass

In an OZI suppressed channel with variable mass glueballs with the right quantum numbers should break down the OZI suppression in the mass regions where they exist, and dominate the reaction channel. Thus the OZI suppression can act as a filter for letting

* The SLAC $\iota(1440)$ is thought to be in a channel where glueballs are enhanced since it is found in J/ψ radiative decay.

** One could for example inadvertently mix states from the basic nonet with those of a radial excitation.

glueballs pass while suppressing other states. Furthermore, the breakdown of the OZI suppression can serve as a clear signal that one or more glueballs are present in the mass region. The basic idea is that according to present concepts in QCD, the OZI suppression is due to the fact that two or more hard gluons are needed to bridge the gap in an OZI disconnected or hairpin diagram,* and the early onset of asymptotic freedom leads to a relatively weak coupling constant for these gluons, which then causes the OZI suppression. On the other hand, if the glue in the intermediate state resonates to form a glueball, the effective coupling constant (as in all resonance phenomena) must become strong, and the OZI suppression should disappear in the mass range of the glueball. This should allow hadronic states with the glueball quantum numbers to form with essentially no OZI suppression. This argument has been made previously by the author at ERICE[5] and elsewhere.[6,13-14] Thus the OZI suppression essentially acts as a filter which lets glueballs pass and suppresses quark states.

THE $\pi^- p \to \phi\phi n$ (OZI FORBIDDEN CHANNEL)

The BNL/CCNY collaboration had shown several years ago that in the OZI forbidden[18] (or suppressed) reaction $\pi^- p \to \phi\phi n$ at an incident pion energy of 22.6 GeV, that the OZI suppression was essentially absent[4] in this OZI forbidden process. This was quantitatively demonstrated, and interpreted by the author as evidence for glueballs in the $\phi\phi$ system.[5,6] However, initially 100, and later 170, events were obtained and this small number did not allow a viable convincing partial wave analysis to explicitly identify the glueball candidates quantum numbers, mass, width, etc. The observed $\phi\phi$ mass spectrum in other later low statistics measurements were consistent with our results.[19]

* Three gluons are needed if the hairpin is a vector, two are needed if the hairpin is a scalar.

However, BNL/CCNY planned a new experiment to obtain > than an order of magnitude more data which would hopefully allow a significant partial wave analysis. In order to accomplish this the BNL MPS (Multiparticle Spectrometer) was being redesigned so that a new novel high speed drift chamber system replaced the spark chambers and thus allowed gathering data at an order of magnitude faster rate.[20]

This spring we successfully commissioned the new MPS II and in a 2-3 week run obtained 1203 $\pi^- p \to \phi\phi n$ events even though the visible cross section is only $\sim$ 6 nanobarns.

A partial wave analysis of this data which was just presented at the Paris Conference,[21] yields two explicit strong glueball candidates in the $\phi\phi$ system with all quantum numbers, mass and width determined. The experiment was done at an incident π^- energy of 22 GeV.

Let us now look at the diagrams in Fig. 1 which represent the various channels studied in the experiment.

The basic reaction observed is given by the OZI allowed reaction (Fig. 1a) $\pi^- p \to K^+K^-K^+K^-n$.

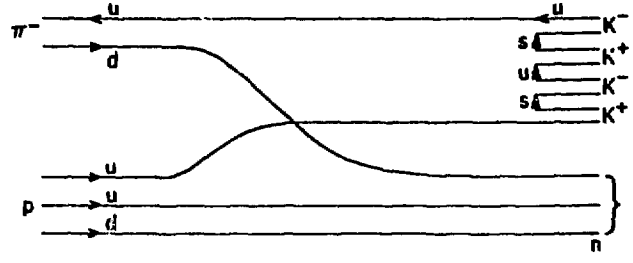

Figure 1a: The quark line diagram for the reaction $\pi^- p \to K^+K^-K^+K^-n$, which is connected and OZI allowed.

In QCD[22] one considers these OZI allowed reactions to proceed by a continuous series of exchanges of single and perhaps some low energy multiple gluons which have relatively strong effective coupling constants and thus proceed as strong interactions. The poorly understood hadronization process can to a large extent occur near the outer regions of the confinement region and have unsuppressed cross sections.

If one K^+K^- pair forms a ϕ we have the reaction $\pi^-p \to \phi K^+K^-n$ (see Fig. 1b) which is still a connected diagram and OZI allowed.

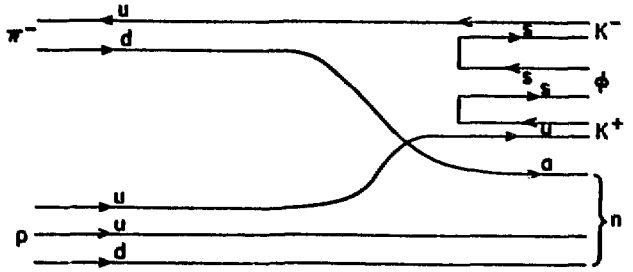

Figure 1b: The quark line diagram for the reaction $\pi^-p \to \phi K^+K^-n$, which is connected and OZI allowed.

However if both K^+K^- pairs form ϕ's we have a disjoint (hairpin) diagram which is OZI forbidden. Thus $\pi^-p \to \phi\phi n$ as shown in Fig. 1c is an OZI forbidden diagram and should exhibit the OZI suppression.

This has been clearly shown for $\pi^-p \to \phi n$ where the OZI suppression factor has been found to be ~ 100.[23] Thus typically one finds

$$\frac{\sigma(\pi^-p \to \omega n}{\sigma(\pi^-p \to \phi n} \sim 100$$

reflecting the OZI suppression factor.

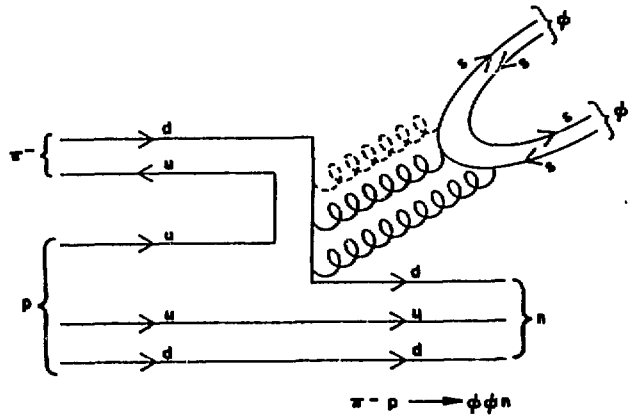

Figure 1c: The quark line diagram for the reaction $\pi^-p \to \phi\phi n$ which is disjoint (i.e. a hairpin diagram) and is OZI forbidden. Two or three gluons are shown connecting the disconnected parts of the diagram depending upon the quantum numbers of the $\phi\phi$ system.

However, another OZI allowed process corresponding to a connected diagram is $K^-p \to \phi\Lambda$. The ratio

$$\frac{\sigma(K^-p) \to \phi\Lambda}{\sigma(\pi^-p) \to \phi n} \gtrsim 60$$

again showing the typical OZI suppression.[24]

The decay matrix element squared of $\phi \to K^+K^-$ (shown in Fig. 2a), an OZI allowed process, is ~ 100 times that for $\phi \to \rho^+\pi^-$ which is OZI suppressed.[18a] Hence in both the production and decay, a single ϕ hairpin (disjoint diagram, see Fig. 2b), corresponds to an OZI suppression factor ~ 100.

Now you may ask is it as legitimate to consider $\pi^-p \to \phi\phi n$ also as a disjoint diagram subject to the OZI suppression. The answer is clearly yes as I shall now demonstrate. Each of the two ϕ's

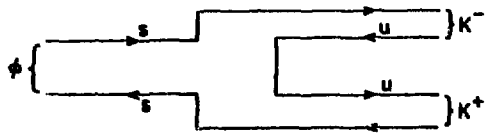

Figure 2a: The quark line diagram for the reaction $\phi \to K^+K^-$ which is connected and thus OZI allowed.

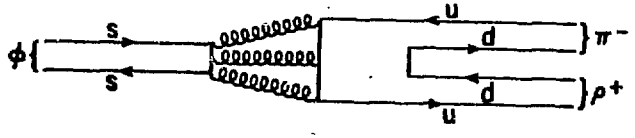

Figure 2b: The quark line diagram for the reaction $\phi \to \rho^+\pi^-$ which is disjoint (i.e. hairpin) and OZI forbidden.

is an almost pure $s\bar{s}$ meson system. If you look at Fig. 1c from right to left you have two $s\bar{s}$ states disjoint from the π^-, p and n part of the diagram which is connected, and contains only u and d quarks. This is basically no different a disjoint diagram than the single ϕ production case (Fig. 2c) where the OZI suppression is

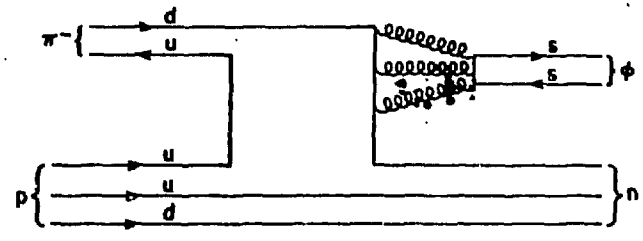

Figure 2c: The quark line diagram for the reaction $\pi^-p \to \phi n$ which is a disjoint (i.e. hairpin) and OZI forbidden.

calculated based on experimental results to be just what is expected from the ϕ decay, a factor $\sim$ 100.

The following is an experimental example of another case where a disjoint diagram formed by two particles in the final state composed of new types of quarks and their antiquarks leads to OZI suppression.[25]

$$\psi(3685) \to J/\psi\,\pi^+\pi^- \ (33 \pm 2)\%, \text{ or } J/\psi\,\pi^0\pi^0 \ (17 \pm 2)\%$$

The full width of the $\psi(3685)$ is 0.215 MeV clearly showing the strong OZI suppression corresponding to the fact that the initial state contains $c\bar{c}$ quarks only, whereas the final state still contains the $c\bar{c}$ quarks but the diagram becomes disconnected when u and d quarks and their antiquarks (to form the two pions) are included in the final state.

But you might say what if I introduce two-step processes or other complicated intermediate states or processes, other than hard multigluons to jump the disjointed part of the diagram. The author has discussed this[6] and shown that the OZI rule is peculiar in that you can defeat it by two-step processes (Fig. 3) or in QCD language changing the nature of the multigluon exchange needed in the one-step diagrams to a series of the ordinary OZI allowed gluon exchanges.

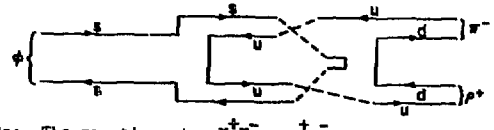

Figure 3a: The reactions $\phi \to K^+K^- \to \rho^+\pi^-$, a two-step connected diagram which appears to be OZI allowed but is not (according to experiment). Proposed cancellations[18b] of artificial nature were proposed to eliminate this problem, but the author believes the simple Ansatz that they are highly suppressed is much more likely to be consonant with observations and QCD.

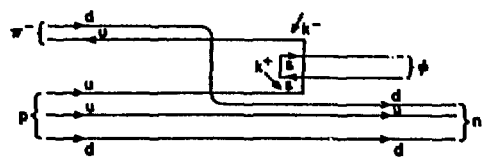

Figure 3b: The reaction $\pi^- p \to K^+ K^- n \to \phi n$, a two-step connected diagram which appears to be OZI allowed but is not (according to experiment).

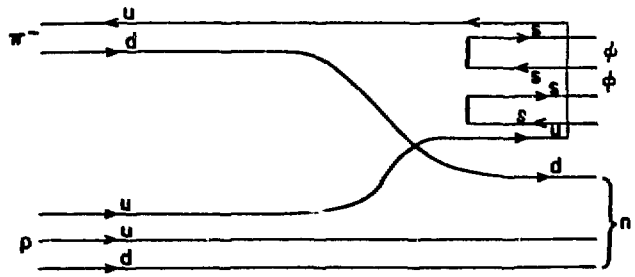

Figure 3c: The reaction $\pi^- p \to \phi K^+ K^- n \to \phi\phi n$ via a two-step connected diagram which appears to be OZI allowed but is not.

In other words, Zweig's diagrams are, based on all experimental observations, to be taken literally as one-step processes and the multigluon exchanges needed to connect disconnected parts of the diagrams are not to be tampered with. Why are these peculiarities observed? I cannot answer that. Neither can I answer why color exists, why confinement? Why quarks? etc. etc. etc. These are all concepts based on observation.

It is certainly consistent with all experimental observations in the ϕ, J/ψ and T systems that the OZI rule[18] works very well,* and as I have pointed out if one wants to invent appropriate multi-step processes or tamper with the nature of a gluon exhcange in the one-step Zweig diagrams one can defeat the rule.** Therefore I assume the OZI rule (with the caveats that I have mentioned) as an input assumption, and of course QCD as an input assumption in drawing my conclusions in this paper. If you grant me QCD and OZI as valid assumptions, I will later conclude that we have discovered one or more glueballs. If you quarrel with assuming QCD, there is absolutely no point in discussing glueballs. If you quarrel with assuming OZI (as caveated) we will have to demote our conclusion of glueball discovery to discovery of strong glueball candidates, and suggest you explain why the assumption of the OZI rule which has been consistently observed to work be replaced by complicated alternatives. Remember the name of the physics game is simplicity when it works.

THE NEW BNL/CCNY $\pi^- p \to \phi\phi n$ EXPERIMENT

We utilized the new BNL MPS II, the experimental arrangement of which is shown in Fig. 4. The major changes from the MPS I experiments to MPS II experiments was to replace the spark chambers with drift chambers with ten times more data-gathering rate capability and to improve the (charged particle and γ) veto box around the liquid hydrogen target to obtain an even cleaner neutron signal.

* The fact that the OZI rule works well for the single ϕ, J/ψ and T is understandable if there are no glueballs with the right quantum numbers at their masses.

** These restrictions apparently violate crossing and unitarity. I consider these peculiarities as another fact of life of quarks, gluons, and color confinement.

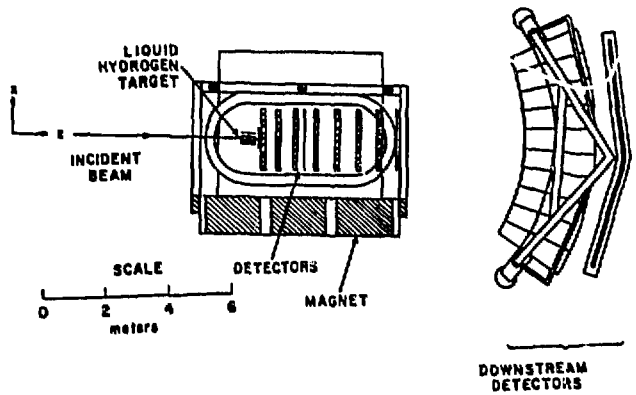

Figure 4: The MPS II and the experimental arrangement (see Ref. 3 for further details).

Figure 5 is a scatter plot of the mass of one K^+K^- pair versus the mass of the second K^+K^- pair. Each event has two points on the plot since there are four possible combinations. One clearly notices the two ϕ bands standing out over the 4-kaon background. However, where the two ϕ bands cross we find a black spot whose peak intensity (corrected for resolution and double counting) is greater than 1,000 times that of the adjoining 4-kaon event intensity. The ϕ band intensity (corrected for resolution) is about a factor of 20 higher than the adjoining 4-kaon event intensity. Where the two ϕ bands cross, the $\phi\phi$ intensity (corrected for resolution) is $\sim$ 50 times greater than the $\phi(K^+K^-)$ intensity. If the OZI suppression were working very little enhancement would be seen here. Thus we have a patent violation of the OZI suppression. This effect was already clearly noted by us in 1978.[4] The speaker has previously shown that if one uses the isobar model,[26] which is well known to work well and has no provision for OZI suppression

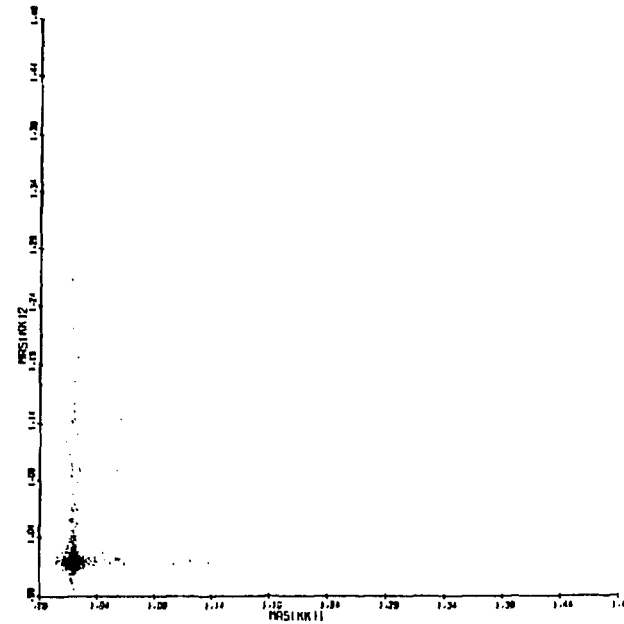

Figure 5: Scatter plot of K^+K^- effective mass, two randomly chosen mass combinations are plotted for each event. Clear bands of $\phi(1020)$ are seen with an enormous enhancement (black spot) where they overlap (i.e. $\phi\phi$).

in it, one can quantitatively explain[5,6] the behavior of this scatter plot within a factor of 2. The new greater statistics experimental data are consistent with the earlier experiment in this regard.

Independent evidence of the breakdown of the OZI suppression is given[27] by a study of the reaction $K^-p \to \phi\phi\Lambda$ or $\phi\phi\Sigma^0$. This is an OZI allowed reaction and yet the cross section obtained is

only a factor ~ 4 larger than the cross section for $\pi^- p \to \phi\phi n$ which is an OZI forbidden reaction. We also have kaons in our beam and have studied this reaction and from preliminary results obtain the same factor ~ 4. One should divide the 4 by a factor of 2 since in the π^- case only n is allowed to accompany the $\phi\phi$, whereas in the K^- case, either a Λ or Σ^0 is accepted.

Thus within a factor of 2 the two cross sections are equal, showing little difference between the OZI allowed and forbidden reactions.

In contrast to this, the ratio[24]

$$\frac{\sigma(K^- p) \to \phi\Lambda}{\sigma(\pi^- p) \to \phi n} \approx 60$$

showing the typical OZI suppression of the forbidden to the allowed reaction, and as is also well known;

$$\frac{\sigma(\pi^- p) \to \omega n}{\sigma(\pi^- p) \to \phi n} \sim 100$$

shows the typical OZI suppression ~ 100.

Hence we have shown in a number of ways that the large OZI suppression ~ 100 expected in single ϕ production is present, whereas that expected in $\phi\phi$ production is broken down to within a factor of 2 of OZI allowed processes which is within the uncertainties of the comparisons. Thus we can clearly conclude on a number of grounds that the expected OZI suppression is essentially entirely absent in the $\pi^- p \to \phi\phi n$ OZI forbidden process. Figure 6 shows the mass spectrum of the other K^+K^- pair in one event whenever one K^+K^- pair falls in the ϕ mass band (1014.6 ± 14 MeV) and clearly indicates the huge $\phi\phi$ signal. Figure 7 shows a very clear neutron recoil from the $\phi\phi$ with an estimated contamination of non-neutron events in our data sample $\sim 3\%$ which should have a negligible effect on our analysis. In the mass region where we did our partial wave analysis, the ϕK^+K^- background was small (approximately 10%) and it was included in our analysis.

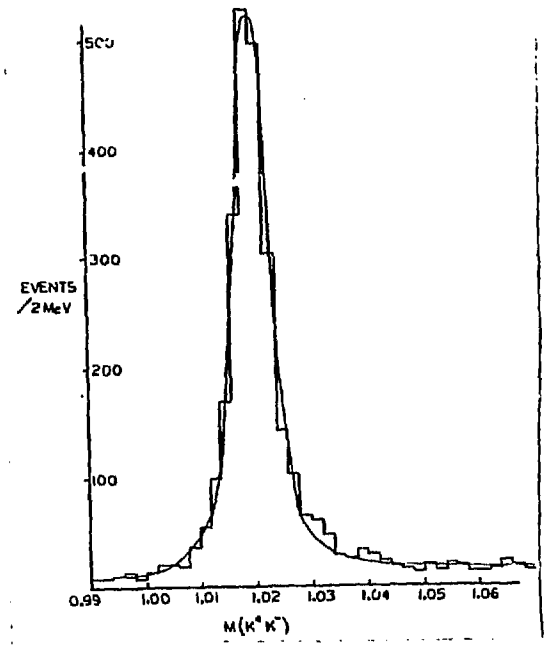

Figure 6: The effective mass of each K^+K^- pair for which the other pair was in the ϕ mass band.

The histogram in Fig. 8 shows the detected $\phi\phi$ effective mass spectrum for 1203 $\pi^- p \to \phi\phi n$ with an estimated background of 130 events from ϕK^+K^- ($\approx 10\%$) and ≈ 40 events of non-neutron recoil. The dashed line is the Monte Carlo determined acceptance of the apparatus of our partial wave analysis solution to be discussed later. However one should note that the result obtained for the acceptance is close to that one would obtain from phase space. Furthermore the results of the partial wave analysis are insensitive to considerable changes in the acceptance. The observed

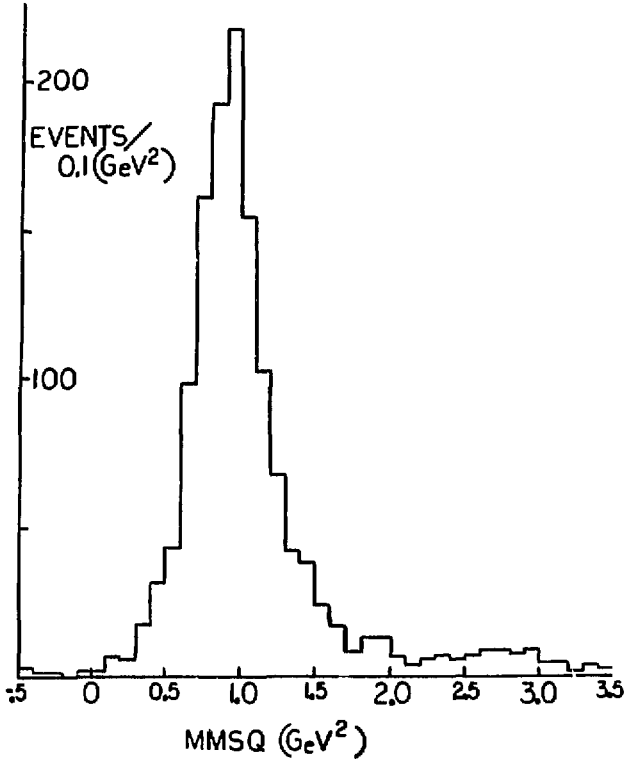

Figure 7: The missing mass squared for the neutral recoiling system from the $\phi\phi$.

spectrum is consistent with that of Ref. 3 and other subsequent low statistics $\phi\phi$ experiments.[19] One should note that the $|t'| \lesssim 0.3$ GeV^2 the t' distribution is consistent with $e^{(9.4 \pm 0.7)t'}$. It

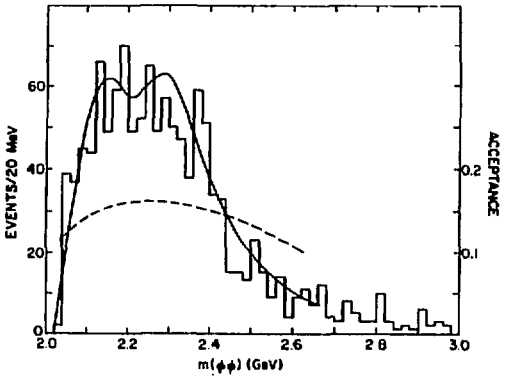

Figure 8: The observed $\phi\phi$ effective mass spectrum. The dashed line is the Monte Carlo calculated acceptance. The solid line is the P.W.A. fit to be discussed later.

should be noted that the $\phi\phi$ mass spectrum from $K^-p \to \phi\phi\Lambda/\Sigma$ [27] is much broader and extends to much higher masses (see Fig. 9).

THE PARTIAL WAVE ANALYSIS

In order to perform the partial wave analysis (PWA) we used six angles to specify all kinematic and other characteristics of the $\phi\phi$ system with each ϕ decaying into a K^+K^- pair.

Figure 10 shows the Gottfried-Jackson frame (which is the rest frame for the $\phi\phi$ system). The usual GJ angles, β(polar) and γ azimuthal, were employed. We then considered the rest frame of each ϕ.

Figure 11 shows the rest frame of ϕ_1. In it we label the polar angle of the decay of the K_1^+ relative to the ϕ direction as θ_1, and the azimuthal angle of the decaying K_1^+ as α_1. There is

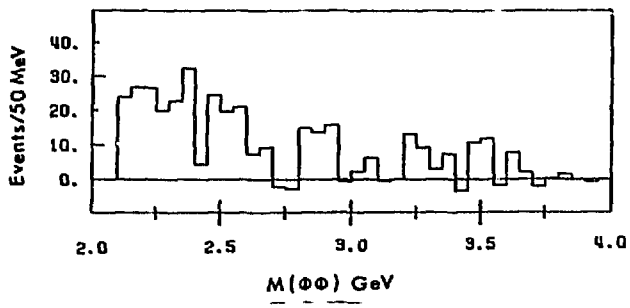

Figure 9: The $\phi\phi$ effective mass spectrum for $K^-p \to \phi\phi\,\Lambda/\Sigma$.

a similar rest frame (not shown) for the second ϕ with corresponding polar angle for K_2^+ of θ_2 and azimuthal angle α_2. Since the azimuthal angles α are the same in either ϕ rest frame, α_2 is shown in the rest frame of α_1. However, of course, θ is different in the two rest frames.

Since the decay kaons are spinless, these six angles specify everything for the $\phi\phi$ system decaying into kaons. These angles and relevant combinations of them were used in the partial wave analysis. For the $\phi\phi$ system, I = 0 and C = +.

The partial waves considered were all waves with J = 0,1,2,3,4; L = 0,1,2,3; S = 0,1,2; $-J \leq M \leq J$, P = ±, η = ± where J is the total angular momentum of the $\phi\phi$ system. L is the orbital angular momentum, M is J_z, P is the parity and η the exchange naturality of the wave.

Due to the identity of the two ϕ mesons bose statistics requires that L + S = even number, and this was an imposed requirement. The above criteria led to a group of 52 independent waves. The maximum likelihood method was used for the PWA. In order to determine the partial waves playing a major role in the $\phi\phi$ system, the events in the mass region 2.1 to 2.3 GeV were fitted with an

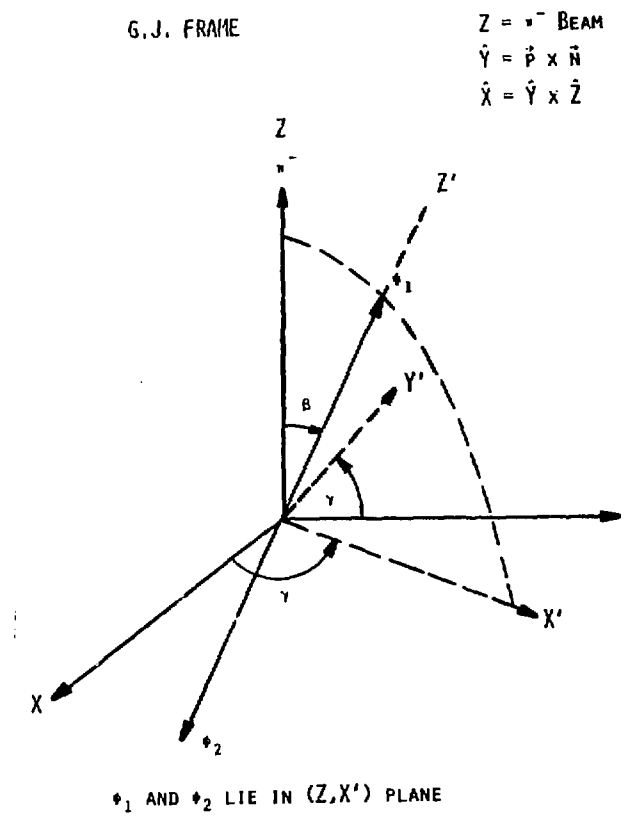

Figure 10: The Gottfried-Jackson frame with polar angle β and azimuthal angle γ.

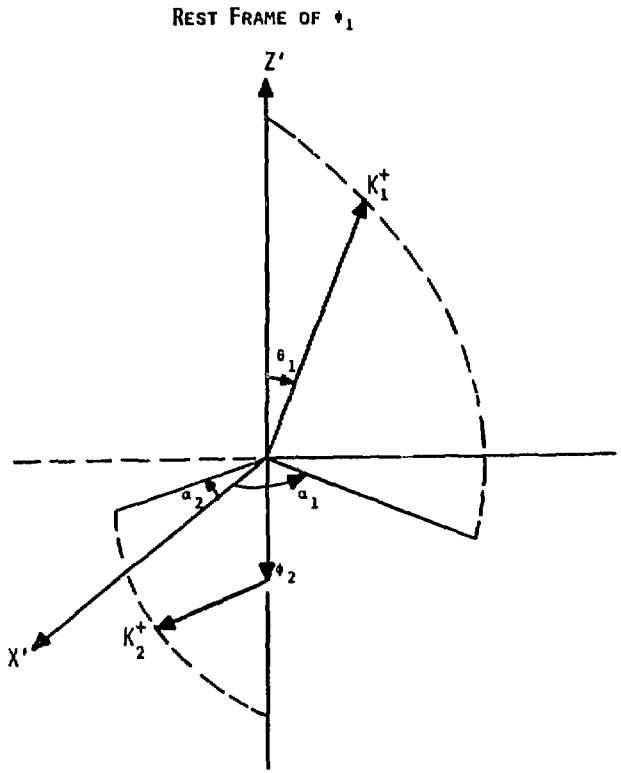

Figure 11: The ϕ rest frame with the polar angle θ_1 of the decay K_1^+ (relative to ϕ direction) and the azimuthal angle a_1 of the decay K_1^+.

incoherent background plus one additional partial wave of specific J^P, S, L, M and η, cycling through each of the 52 waves described above. The largest, and only significant contribution came from $J^{PC}SLM^\eta = 2^{++}200^-$. This wave was retained and in order to search for other waves each of the other 51 were added one at a time in turn. The only significant additional contribution came from $J^PSLM^\eta = 2^+220^-$. These two waves were then retained and each of the remaining fifty were added one at a time in turn. No significant contribution from any other wave was found. The $\phi\phi$ data were then divided up into five adjoining 100 MeV wide bins starting from threshold, so that we could explore the mass dependence of the partial wave structure. The bin size was chosen because about 200 events per bin are needed to obtain reliable solutions.

The background from ϕK^+K^- events ($\approx$ 11%) was estimated from an examination of the regions adjacent to the $\phi\phi$ peak. There was no evidence of any angular structure, so this background was represented by a flat distribution in all angles. A maximum likelihood fit to the five bins using the two $J^P = 2^+$ waves described gave a very good fit with $\chi^2/D.F. \lesssim 1$ when the statistics and systematic errors were considered. To ensure that no other combination of two waves would give an equivalent fit, each possible combination of two waves, i.e. 52 x 51/2 = 1326, were tried in the central bin where the S and D waves found had a significant overlap. The closest one came to a fit was 5σ away from the original fit. These $\sim 5\sigma$ fits always involved the S-wave originally found as one of the two waves. Hence the original two-wave fit is clearly selected.*

Therefore the mass independent solutions (i.e. no parameterization chosen) for the $J^PSLM^\eta = 2^+200^-$ S-wave and the 2^+220^- D-wave are shown in Fig. 12. The lower half of the figure shows the $|S|^2$

* One might perhaps expect a background of the L = 0, $J^P = 0^+$ wave at threshold, but this wave contributes only 10 ± 5% of the events in the lowest mass bin. Furthermore one should recall backgrounds do not break down OZI suppression.

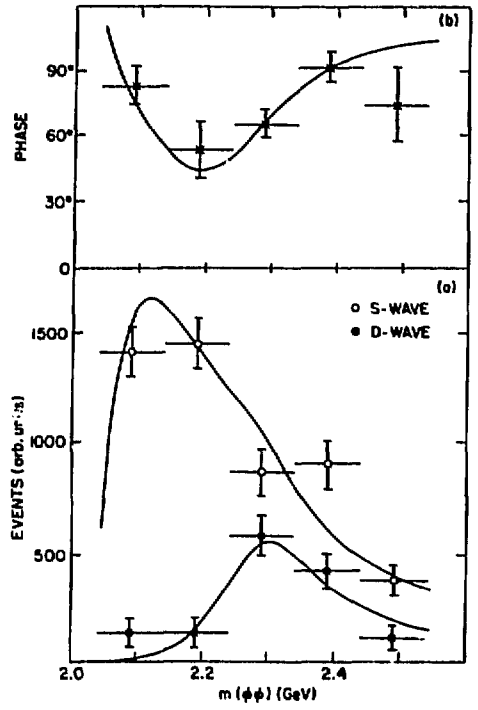

Figure 12: (a) The points show the intensity ($|S|^2$ and $|D|^2$) and for the best mass-independent two-wave fit described in the text.
(b) The D-S phase difference (mass-independent) for the best two-wave fit described in the text. The curves show the resultant best maximum likelihood fits for the parameterization of two interfering Breit-Wigner resonances.

normalized to events as the open circle points and the corresponding $|D|^2$ amplitudes squared are shown as the closed points. The x points on the top part of the figure show the D-S phase difference. A natural parameterization for these data is one or two Breit-Wigners. A one Breit-Wigner fit was rejected by > 10σ, primarily because of the phase difference. A two Breit-Wigner fit on the other hand was very good with $\chi^2/DF \approx 1$. The solid lines show this fit and the quantum numbers and parameters of the two resonances to be discussed later are shown in Table I.

TABLE I

Quantum numbers and parameters of the Breit-Wigner resonance fit to the S- and D-wave amplitudes (and phase difference) of Fig. 12.

	$g_T(2160)$	$g_T(2320)$
$I^G J^{PC}$	0^+2^{++}	0^+2^{++}
Mass (GeV)	2.16 ± 0.05	2.32 ± 0.04
Γ_{tot}	0.31 ± 0.07	0.22 ± 0.07
Ratio of Partial Widths	$\Gamma_D/\Gamma_S \approx 0.02$	$\Gamma_S/\Gamma_D \approx 0.04$

It at first appears remarkable that we can demonstrate such selectivity (i.e. 2 waves selected out of 52). However this results from the fact that the φφ system is a very powerful analysis system for picking particular waves. In order to see how this comes about let us look at Figs. 13a and 13b where angular variables for numerous allowed (i.e. L + S = even) pure waves up to $J^{PC} = 4^{++}$ are shown. Our data shows a flat distribution in γ, all M = 0 waves which are shown have this feature. Therefore there is no need to plot γ.

We can notice from these figures which show the behavior of α, $\alpha_1' - \alpha_2'$, $\alpha_1' + \alpha_2'$, cosβ, cosθ, $\cos\theta_1' + \cos\theta_2'$, $\cos\theta_1' - \cos\theta_2'$, that each wave has its own characteristic signature in the various variables shown. The primes (i.e. $\alpha_1' - \alpha_2'$) were modifications to

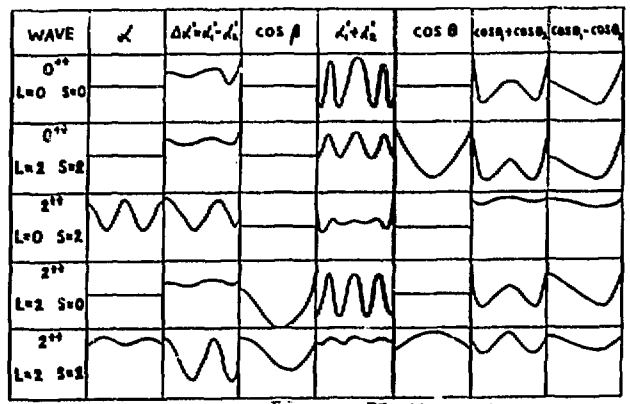

Figure 13a: Various pure waves from $J^{PC}=0^{++}$ to $J^{PC}=2^{++}$ with M = 0.

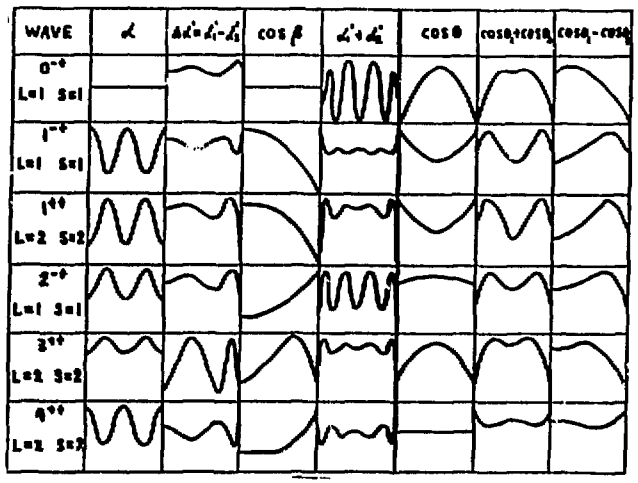

Figure 13b: Various pure waves from $J^{PC}=0^{-+}$ to $J^{PC}=4^{++}$ with M = 0.

the variables for display and comparison purposes so as to equalize the phase space in each histogram bin (to be shown later). For example

$$\Delta\alpha' = \frac{(\alpha_1 - \alpha_2)}{\pi} \quad \frac{(1 - |\alpha_1 - \alpha_2|)}{4\pi} .$$

Similar equalitations in phase space were made per bin wherever primes are shown. Due to the inherent symmetry, cosβ, $\Delta\alpha' = \alpha'_1 - \alpha'_2$, and $\cos\theta'_1 - \cos\theta'_2$ have been folded, the data for α_1 and α_2 added, and the data for $\cos\theta_1$ and $\cos\theta_2$ added. The very characteristic signature for particular pure waves in these angular variables give us the great selectivity we have found. For example, notice that the two $J^P = 2^+$ (S and D) waves that we have found in the partial wave analysis (the third and the fifth from the top in Fig. 13a) have similar very characteristic large structure in $\alpha'_1 - \alpha'_2$ and the S-wave has a characteristic structure in α whereas the D-wave does not. Thus $\alpha'_1 - \alpha'_2$ and α are the most important variables in selecting the $J^P = 2^+$ waves we found in our partial wave analysis.

With this introduction I now turn to a detailed comparison (in 3 mass bins) of the data and the Monte Carlo generated prediction for our fit from the partial wave analysis. The Monte Carlo results are acceptance-corrected and are based on over 14,000 events, more than an order of magnitude more statistics than the data (for which the actual number of events are shown in the plots). Thus the statistical fluctuations in the Monte Carlo results will be small compared to those in the data. Furthermore we determined that the angular variables and correlations were not sensitive to the acceptance except in the case of the G.J. angle β.

Figure 14a shows a comparison of the data and Monte Carlo for ϕ (the G.J. azimuthal angle) and the polar angle θ. The agreement is excellent.

Figure 14b shows a comparison of the data and Monte Carlo for cosβ, where β is the G.J. polar angle. Even though cosβ is sensitive to the acceptance, we obtain a quite reasonable agreement.

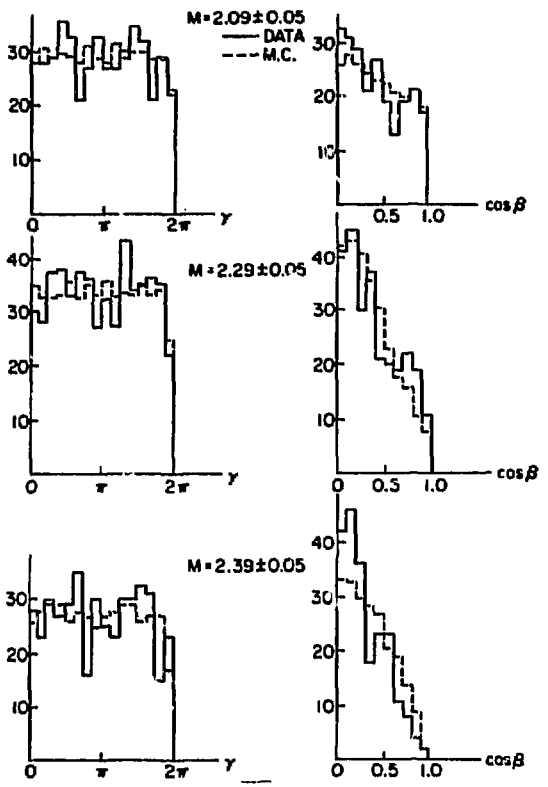

Figure 14: (a) Comparison of the data and the acceptance-corrected Monte Carlo for the fit in G.J. azimuthal angle γ.
(b) Comparison of the data and the acceptance-corrected Monte Carlo for the fit in G.J. polar angle function cosβ.

Figure 15 shows the data and Monte Carlo predictions of the fit for α and $\Delta\alpha' = \alpha_1' - \alpha_2'$. The agreement between the data and the Monte Carlo prediction based on the fit is most impressive for $\Delta\alpha'$ since there are large factors $\gtrsim 3$ between peaks and valleys.

In the case of α the agreement is also quite good. The first bin shows large structure, characteristic of the S-wave, as we have remarked previously. The next bin shown (third bin) is where the D-wave is very important and shows very little structure in α_1, which, as we pointed out previously, is a feature of the D-wave. The agreement is good. The next bin shows the structure returning as the D-wave drops down and again indicating good agreement.

Figure 16 shows the comparison of the data with the Monte Carlo for $\alpha_1' + \alpha_2'$ and $\cos\theta$. Here again the agreement is generally quite good and there is no sizeable structure in these variables.

Figure 17 shows the comparison with the Monte Carlo for $\cos\theta_1' - \cos\theta_2'$ and $\cos\theta_1' + \cos\theta_2'$. Here again the agreement is quite good and there is no sizeable structure in these variables.

Thus we have made ten* characteristic angular correlations for six independent variables and found good agreement - striking at times in $\Delta\alpha'$ and α for example. The data and Monte Carlo agree in all mass bins in all variables.

The next question is how does our fit compare with the observed $\phi\phi$ mass spectrum? This is shown in Fig. 18 where the solid line is the fit prediction. The agreement here is also quite good. However, I must remark that in dealing with the $\phi\phi$ system, its myriad and characteristic angular distributions and angular correlations are much more important tests of the significance of the fit, than the mass spectrum. Thus we can feel quite confident that our two Breit-Wigner fits are in excellent agreement with the data.

* α represents the data for α_1 and the data for α_2 added due to symmetry. Cosθ represents the data for $\cos\theta_1$ and the data for $\cos\theta_2$, added due to symmetry.

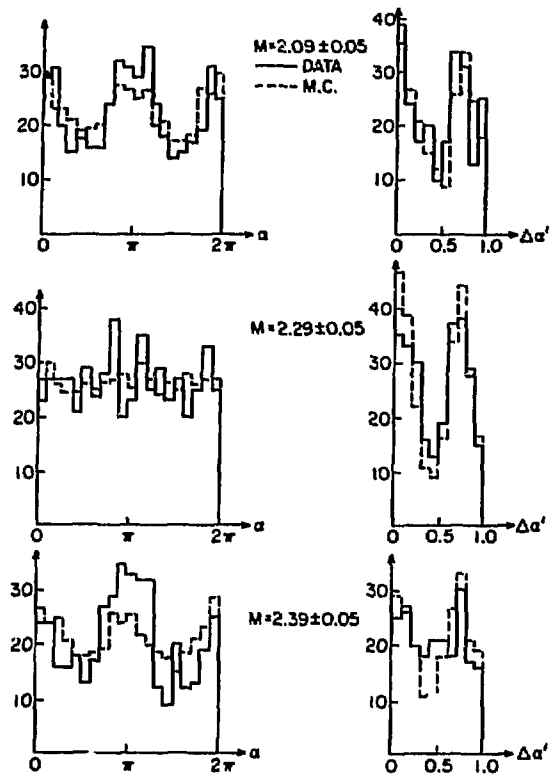

Figure 15: (a) Comparison of the data and the acceptance-corrected Monte Carlo for the azimuthal angle α of the decay K^+ in the ϕ rest frame.
(b) Comparison of $\Delta\alpha' = \alpha_1' - \alpha_2'$ with the acceptance-corrected Monte Carlo for the fit.

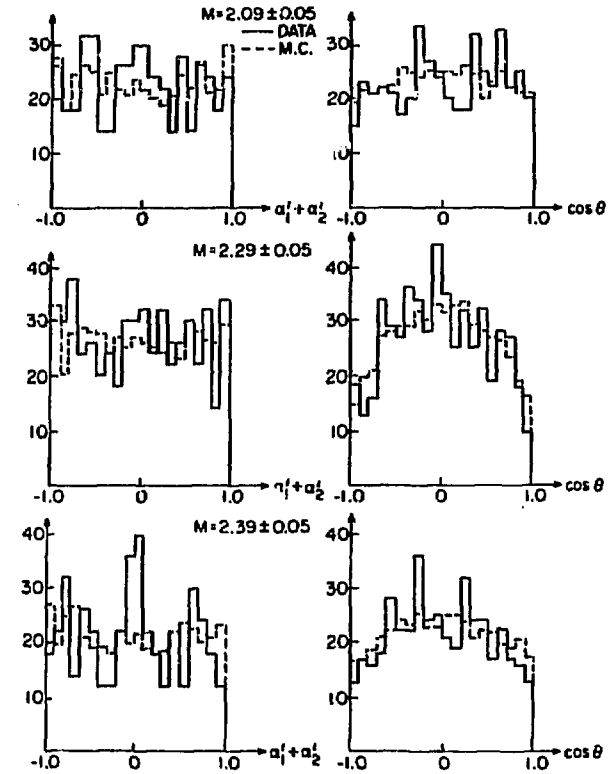

Figure 16: (a) Comparison of the data and the acceptance-corrected Monte Carlo for $\alpha_1' + \alpha_2'$.
(b) Comparison of the data and the acceptance-corrected Monte Carlo for $\cos\theta$.

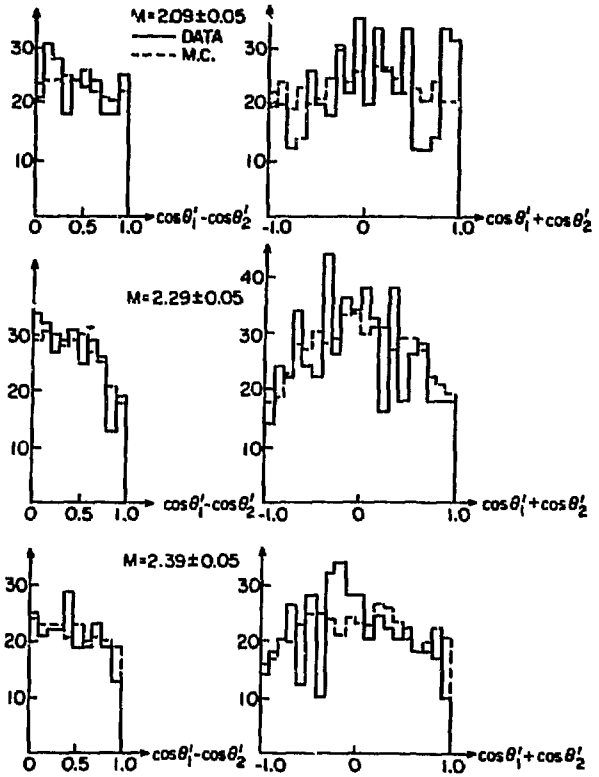

Figure 17: (a) Comparison of the data and the acceptance-corrected Monte Carlo for $\cos\theta_1' - \cos\theta_2'$.
(b) Comparison of the data and the acceptance-corrected Monte Carlo for $\cos\theta_1' + \cos\theta_2'$.

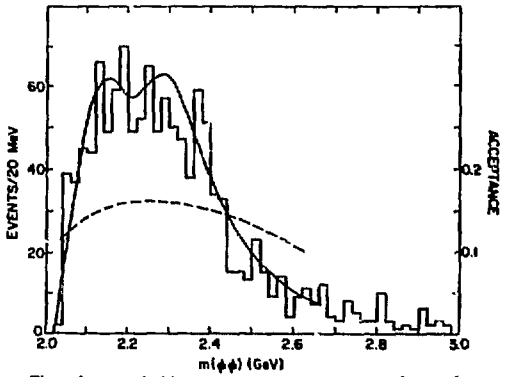

Figure 18: The observed $\phi\phi$ mass spectrum compared to the predicted (solid line curve) mass spectrum from the acceptance-corrected fit. The dashed line is the acceptance.

The mass and full width, partial width ratios, and all the quantum numbers for these two Breit-Wigner resonances are given in Table I. They are at the very least strong glueball candidates due to the breakdown of the OZI suppression, and the striking selectivity of 2 out of 52 possible waves selected.

In fact if one assumes:

1. The correctness of QCD;

2. The universality of the OZI rule (with the necessary caveats) as described previously. Namely, the necessary one-step requirement which is equivalent to the requirement that there is no change in the nature of a gluon exchange. The above is equivalent to the statement that a disjoint Zweig diagram, due to introduction of a new type of $q\bar{q}$ pairs, must involve a multigluon exchange. This leads to OZI suppression due to a weakly coupled multigluon exchange. As I have pointed out previously, a glueball in which the gluons resonate would lead to effectively strongly-coupled glue, and break down the OZI suppression.

This leaves me as the only explanation of the OZI suppression breakdown and the observed selectivity the presence of one or two primary glueballs in the mass region with these quantum numbers. Impure $q\bar{q}$ intermediate states, 4 quark states, etc. are ruled out by the above assumptions (assumption 2).

Why do I say one or two primary glueballs? Because one primary gluebull could break down the OZI suppression and possibly mix with a nearby quark state with the same quantum numbers yielding two states very rich in resonating glue. Of course both states could come from different primary glueballs* since we expect that there is a glueball spectrum of states - not just a single glueball.

It should be noted that in a number of papers it was concluded that the width of a glueball should be narrower than hadronic resonances typically by a factor $\sim \sqrt{\text{OZI suppression factor}}$. These considerations were based on treating the quark-glue, glue-glue coupling as weak, and clearly do not apply if the glue-glue coupling becomes strong enough to form a resonance, in which case we are generally dealing with a very strongly interacting multigluon resonance.

In fact the glue-glue coupling is effectively stronger than the quark-glue coupling, and therefore, glueballs should be as wide, or wider than, typical hadronic resonances in the mass region.

In Table II we list some typical resonance widths from the particle data group tables and widths for other glueball candidates. We see that $\Gamma \sim (200\text{-}300) \pm 100$ MeV are reasonable values for glueballs.

MASS AND J^{PC} OF THE GLUEBALLS FROM VARIOUS PHENOMENOLOGICAL APPROACHES

In constituent glueball models[12] due to confinement, the gluon is considered to have an effective mass $m_g \gtrsim 0.75$ GeV.[28]

* They might also eventually dress themselves to some degree with $q\bar{q}$ pairs.

TABLE II

Past Resorance Widths for Some Hadronic Resonances from the Particle Daca Group Table[25]

State	$I^G(J^P)C_n$	Full Width Γ in MeV
g(1690)	$1^+(3^-)^-$	200 ± 20
ρ'(1600)	$1^+(1^-)^-$	300 ± 100
f(1270)	$0^+(2^+)^+$	179 ± 20
Resonance Widths for Other Glueball Candidates[9,10,15]		
SLAC ι(1440)	$(0^-)+$	55^{+20}_{-30}
θ(1640)	$(2^+)+$	220^{+100}_{-70}
BNL/CCNY $g_g(1240)$	$0^+(0^{++})$	140 ± 10

Thus we might expect to be in the three-gluon sector. One should note that due to the self-coupling between the gluons and their splittings that a gauge invariant description with a definite number of gluons is not possible. Nevertheless it is physically appealing and reasonable to expect in constituent gluon models that the lowest lying ground state would be mostly composed of 2 gluons and have a mass $\gtrsim 2 \times 0.75$ GeV $\gtrsim 1.5$ GeV. One would expect another ground state in the 3g sector mostly composed of 3 gluons with a mass $\gtrsim 3 \times 0.75$ GeV $\gtrsim 2.25$ GeV.

The MIT bag calculations of glueballs[29] assume massless gluons and obtain predictions for quantum numbers and masses of various states.[29] The masses do not fit some present glueball candidates. Hyperfine energy shifts that depend on α_s have been put into the bag calculations to allow such fits.[30] Adapting these methods, we have derived m_g for two-gluon states as a function of α_s. The SLAC ι(1440) and θ(1640) glueball candidates, and the BNL/CCNY $g_g(1240)$ glueball candidate, were used as inputs to derive the results shown in Fig. 19. As you can see, we can obtain a $J^{PC} = 2^{++}$ $g_T(2160)$ at about the right mass as an excited state in the 2g

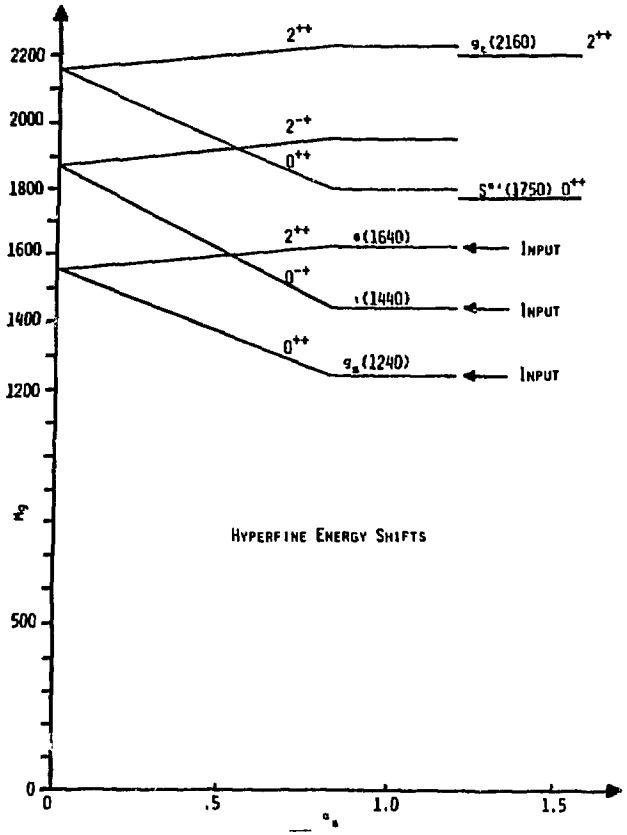

Figure 19: The predicted mass and quantum numbers of the 2g glueballs from adopting the methods of Ref. 30. The $\iota(1440)$, $\theta(1640)$ and $g_B(1240)$ were used as input to determine the overall mass level, the spacing between the levels, and α_s (till break in lines).

sector.* However, the massless assumption for gluons in the bag does not allow $J^{PC} = 2^{++}$ for low-lying 3-gluon states, in contrast to the constituent gluon model which allows all J^{PC} for 3g states and all J^{P+} (i.e., $C = +$) for 2g states.

So far, lattice calculations[31] have concentrated mainly on the glueball ground state getting $J^{PC} = 0^{++}$, $M \sim 0.8 - 1.0$ GeV. Recently they have begun to attack higher spin states.[31] The work is still preliminary, but indications are that higher spin states could well show up in our mass region. Thus, in summary, one finds that the phenomenological models are generally compatible with our results, except for the possibility of the MIT bag calculations if we are in the 3g sector.

CONCLUSIONS

Given QCD as an Ansatz and OZI (with appropriate restrictions) as a second Ansatz, I conclude we have discovered either two glueballs with characteristics described below, or two states very rich in resonating glue formed from one primary glueball mixing with a nearby quark state of the same quantum numbers, thus forming two states.

The quantum numbers and characteristics of these states are:

	I^G	J^{PC}	Mass (MeV)	Γ (MeV)
$g_T(2160)$	0^+	2^{++}	2160 ± 50	310 ± 70
$g_T(2320)$	0^+	2^{++}	2320 ± 40	220 ± 70

* However, one should be aware that perturbative treatments are not justifiable at high values of α_s.

REFERENCES

1. C.N. Yang and R.L. Mills, Phys. Rev. 96, 191 (1954).
2. a) Fritzch and Minkowski, Nuovo Cimento 30A, 393 (1975).
   b) R.P. Freund and Y. Nambu, Phys. Rev. Lett. 34, 1645 (1975).
   c) R. Jaffe and K. Johnson, Phys. Lett. 60B, 201 (1976).
   d) Kogut, Sinclair and Susskind, Nucl. Phys. B114, 199 (1975).
   e) D. Robson, Nucl. Phys. B130, 328 (1977).
   f) J. Bjorken, SLAC Pub. 2372.
3. A. Etkin, J.J. Foley, J.H. Goldman, W.A. Love, T.W. Morris, S. Ozaki, E.D. Platner, A.C. Saulys, C.D. Wheeler, E.H. Willen, S.J. Lindenbaum, M.A. Kramer, U. Mallik, Phys. Rev. Lett. 40, 422 (1978).
4. A. Etkin, K.J. Foley, J.H. Goldman, W.A. Love, T.W. Morris, S. Ozaki, E.D. Platner, A.C. Saulys, C.D. Wheeler, E.H. Willen, S.J. Lindenbaum, M.A. Kramer and U. Mallik, Phys. Rev. Lett. 41, 784 (1978).
5. S.J. Lindenbaum, Hadronic Physics of $q\bar{q}$ Light Quark Mesons, Quark Molecules and Glueballs. Lecture presented at XVIII Course: The High Energy Limit, 31 July - 11 August 1980, The International School of Subnuclear Physics, Erice (to be published in proceedings); Also BNL 28498, October 1980.
6. S.J. Lindenbaum, Il Nuovo Cimento, 65A, 222 (1981).
7. P. Fishbane, Glueballs, A Little Review. Talk presented at the 1981 ORBIS Scientiae, Ft. Lauderdale, Florida (to be published).
8. D.L. Scharre, Glueballs, A Status Report, ORBIS Scientiae 1982, Miami, Florida (to be published), and SLAC Report 2880 (1982).
9. D. Antreasyan, Y.F. Gu, J. Irion, W. Kollman, M. Richardson, K. Strauch, K. Wacker, A. Weinstein, D.A. Schman, T. Burnett, H. Cavalli-Sforza, D. Coyne, C. Newman, H.P. Sadrozinski, D. Gelphman, R. Hofstadter, R. Horisberger, L. Kirkbride, H. Kolanoski, K. Konigsman, R. Lee, A. Liberman, J. O'Reilly, A. Osterheld, B. Pollock, J. Tompkins, E.D. Bloom, F. Bulos,

REFERENCES (continued)

Ref. 9 (continued)
R. Chestnut, J. Gaiser, G. Godfrey, C. Kiesling, W. Lockman, M. Oreglia and D.L. Scharre, Phys. Rev. Lett. 49, 259 (1982).

10. a) M. Chanowitz, Phys. Rev. Lett. 46, 981 (1981).
    b) C.E. Carlson, J. Coyne, P.M. Fishbane, F. Gross and S. Meshkov, Phys. Lett. 98B, 110 (1981).
11. J.F. Donoghue, K. Johnson and B. Li, Phys. Lett. 99B, 416 (1981).
12. a) C. Carlson, J. Coyne, P. Fishbane, F. Gross, S. Meshkov, Phys. Rev. D23, 2765 (1981).
    b) J. Coyne, P. Fishbane and S. Meshkov, Phys. Lett. 91B, 259 (1980); C. Carlson, J. Coyne, P. Fishbane, F. Gross and S. Meshkov, Phys. Lett. 99B, 353 (1981).
13. S.J. Lindenbaum, Proc. Sixteenth Rencontre De Moriond, "New Flavours and Hadron Spectroscopy," Vol. II, pg. 187, Ed., J. Tran Thanh Van (Editions Frontieres, France, 1981); H.J. Schnitzer, ibid. pg. 648; K.R. Schubert, ibid. pg. 635.
14. S.J. Lindenbaum, "Evidence for Glueballs", Proc. 1981 EPS Int. Conf. on High Energy Physics, July 9-15, 1981 (Calouste Gubenkian Foundation, Av. Berne, Lisbon, Portugal) (to be published); F.E. Close, "Glueballs, Hemaphrodites and QCD Problems for Baryon Spectroscopy", ibid.
15. A. Etkin, K.J. Foley, R.S. Longacre, W.A. Love, T.W. Morris, S. Ozaki, E.D. Platner, V.A. Polychronakos, A.C. Saulys, Y. Teramoto, C.D. Wheeler, E.H. Willen, K.W. Lai, S.J. Lindenbaum, M.A. Kramer, U. Mallik, W.A. Mann, R. Merenyi, J. Marraffino, C.E. Roos, M.S. Webster, Phys. Rev. D25, 2446 (1982).
16. E. Bloom, talk presented at the XXI Int. Conf. on High Energy Physics, Paris, France, July 26-31, 1982 (to be published); J. Donoghue, ibid.

17. a) J.F. Donoghue, Experimental Meson Spectroscopy - 1980, Sixth Int. Conf., Brookhaven National Laboratory, April 25-26, 1980, Eds. S.U. Chung and S.J. Lindenbaum, AIP Conf. Proc. #67, Particles and Fields Subseries #21, pg. 1040.
b) G. Bhanot, Phys. Lett. 101 B, 95 (1981).
c) G. Bhanot and C. Rebbi, Nuc. Phys. B180, 469 (1981).
d) H. Hamber and G. Parisi, Phys. Rev. Lett. 47, 1792 (1981).

18. a) S. Okubo, Phys. Lett. 5, 165 (1963); G. Zweig, CERN Report TH 401 and 412 (1964); J. Iizuba, Prog. Theor. Phys. Suppl. 37-38, 21 (1966); J. Iizuba, K. Okuda and O. Shito, Prog. Theor. Phys. 35, 1061 (1966); S. Okubo, "A Survey of the Quark Line Rule," Univ. Rochester Report UR 641 (1977).
b) S. Okubo, Phys. Rev. D 16, 2336 (1977).
c) T. Applequist, K. Kane and M. Barnett, Ann. Rev. Nucl. Sci. 28, 387 (1978).
d) I.J. Muzinich and F.E. Paige, Phys. Rev. D 21, 1151 (1980).
e) S.J. Lindenbaum, "Quark Line Diagrams, Rules, and Some Recent Data", BNL 50812 (December 1977).

19. T.A. Armstrong et al., Nucl. Phys. B 196, 176 (1982); C. Daum et al., Phys. Letts. 104B, 246 (1981). The narrow enhancement in ϕ pairs produced from Be as reported in the latter paper is not confirmed by higher statistics results reported by C. Daum et al., and by B.R. French et al. at the XXI Int. Conf. on High Energy Physics, Paris, France, July 26-31, 1982 (to be published).

20. S. Eiseman, A. Etkin, K.J. Foley, R.S. Longacre, W.A. Love, T.W. Morris, S. Ozaki, E.D. Platner, V.A. Polychronakos, A.C. Saulys, C.D. Wheeler, S.J. Lindenbaum, M.A. Kramer, Y. Teramoto. "The MPS II Drift Chamber System", paper submitted to the IEEE 1982 Nuclear Science Symposium, October 20-22, 1982, Washington D.C. (to be published in IEEE Trans. on Nucl. Sci.).

21. S.J. Lindenbaum, C. Chan, A. Etkin, K.J. Foley, M.A. Kramer, R.S. Longacre, W.A. Love, T.W. Morris, E.D. Platner, V.A. Polychronakos, A.C. Saulys, Y. Teramoto, C.D. Wheeler, "A New Higher Statistics Study of $\pi^- p \to \phi\phi n$ and Evidence for Glueballs". Paper presented at the XXI Int. Conf. on High Energy Physics, Paris, France, July 26-31, 1982 (to be published).

22. H. Fritzch and M. Gell-Mann, XVI Int. Conf. on High Energy Physics, Chicago-Batavia, 1972, Vol. 2, p. 135; H. Fritzch, M. Gell-Mann and H. Leutwyler, Phys. Lett. 47B, 365 (1973); S. Weinberg, Phys. Rev. Lett. 31, 494 (1973); S. Weinberg, Phys. Rev. D8, 4482 (1973); D.J. Gross and F. Wilczek, ibid, 3633 (1973).

23. D. Cohen et al., Phys. Rev. Lett. 38, 269 (1977).

24. D.S. Ayres et al., Phys. Rev. Lett. 32, 1463 (1974).

25. Particle Data Group Tables, Phys. Letts. 111B, 12 (1982).

26. S.J. Lindenbaum and R.M. Sternheimer, Phys. Rev. 105, 1874 (1957); 106, 1107 (1957); 109, 1723 (1958); 123, 333 (1961).

27. T. Armstrong et al., CERN EP/82-103 (1982).

28. G. Parisi and R. Petronzio, Phys. Lett. 94B, 51 (1980).

29. J.F. Donoghue, K. Johnson and Bing An Li, CTP #891 UN HEP-139 October 1980.

30. T. Barnes, F.E. Close and S. Monoghan, Phys. Lett. 110B, 159 (1982).

31. C. Rebbi, talk presented at the XXI Int. Conf. on High Energy Physics, Paris, France, July 26-31, 1982 (to be published).